Designing Ring-Current Patterns: [10,5]-Coronene, a Circulene with Inverted Rim and Hub Currents

Guglielmo Monaco,[†] Rosario G. Viglione,[†] Riccardo Zanasi,*[,†] and Patrick W. Fowler[‡]

Dipartimento di Chimica, Università di Salerno, via A. Allende, 84081 Baronissi (SA), Italy, and Department of Chemistry, University of Sheffield, Sheffield S3 7HF, U.K.

Received: January 4, 2006; In Final Form: April 5, 2006

In an axial magnetic field, coronene, corannulene and kekulene support disjoint paratropic-hub and diatropic-rim ring currents. Bond-order and orbital arguments suggest [10,5]-coronene, $C_{30}H_{10}$, comprising 10 fused pentagons around a central decagon, as a system that should support an inverted diatropic-hub/paratropic-rim pattern of induced currents. The proposal is verified by ipsocentric ab initio mapping of currents, reproduced with the economical pseudo-π method, thus validating a powerful toolkit for design of (induced) molecular magnets.

1. Introduction

Newly available methods[1−14] for reliably computing, for visualizing and especially for interpreting[15,16] current-density maps have revealed the complex patterns of current that can form when molecules are subjected to external magnetic fields. Coronene and corannulene, for example, have been shown[17] to support counter-rotating rim and hub currents, with diatropic flow on the outer perimeter and paratropic flow on the central ring. Opposition of circulations follows from the circulene topology of these molecules, and in the ipsocentric picture[15,16] can be attributed to the simultaneous presence of translationally and rotationally allowed $\pi-\pi^*$ virtual excitations. Kekulene and nonplanar [7]circulene also support counter-rotating currents with the diatropic component on the outside of the molecule.[18,19] Buckminsterfullerene provides a three-dimensional example of circulene-like patterns.[20]

Given that ring-currents modulate molecular magnetic properties and that we have a theoretical toolkit for the prediction of ring-current patterns, it is interesting to consider now the possibility of designing molecules with unusual distributions of currents. In particular, as all the rim/hub maps studied so far show a diatropic exterior, would it be possible to invert the pattern and produce a molecule with a paratropic exterior and a diatropic interior? Since, by their origin in virtual excitations between near-degenerate frontier orbitals, paratropic currents are usually intense,[21] a molecule with an extensive paratropic perimeter could be expected to display unusual magnetic properties, which could be relevant for possible materials applications. This paper presents an example of a planar molecule that occupies a local minimum on the potential surface, and hence is predicted to have some stability, but inverts the circulene pattern of counter-rotating currents to give a dominant paratropic (anti-aromatic) perimeter circulation. This molecule is 4,14,3-methyno-2,5-[1]propen[1]yl[3]ylidenebiscyclopenta-[5,6]pentaleno[1,2-*a*:2′,1′-*f*]pentalene, known more simply as [10,5]-coronene. Its unusual properties are shown to be consistent with the orbital model, and reproducible in a simplified "pseudo-π" approximation, giving clues for the further exploitation of these ideas in molecular design.

2. Design Considerations

The target is to find a π system based on a circulene-like template, planar like coronene, but with an inverted pattern of currents. Counter-rotation in ring-current maps of [n]-circulenes can be understood in various ways. At the quantum chemical level, opposition of inner and outer circulations arises from the symmetries and special distributions of orbital excitations.[15,16] This opposition is also predicted by a simple graph-theoretical argument. In the typical circulene topology, a central *n*-ring is surrounded by a belt of *n* equivalent fused rings of size *m*. The external rings can be seen in a mechanical analogy as independent "cogs" driving the circulation in the central ring. If each external ring supports a diatropic current, then simple vector addition yields a diatropic perimeter circulation, vanishing current along the "spokes" of the molecular "cartwheel", and a paratropic inner circulation (see Figure 1). Coronene and corannulene both have $m = 6$ and follow this pattern.[17] Conversely, if the external rings were instead to be paratropic, an inverted pattern would be expected. The examples of pyracylene[22,23] and the fullerenes,[24,25] among others, suggest using pentagonal rings in the belt to provide this inversion. Geometrical considerations based on equilateral polygons show that if $m = 5$ then, for planarity, $n = 10$. Thus, we are led to the molecule $C_{30}H_{10}$, known as [10,5]-coronene (**1**), where 10 pentagonal rings surround a central decagon.[26]

This molecule has four Kekulé structures, corresponding to the pairings of the two conjugated structures of the inner 10- and outer 20-cycles of carbon atoms. In all four, the radial 5/5 graph edges are single bonds, and hence of Pauling π bond order 0, compared to $^1/_2$ for the bonds of the central and perimeter cycles. Thus, inner and outer circuits are decoupled, suggesting an annulene-within-an-annulene (AWA) picture of the electronic structure.[27] The respective $(4n + 2)$ and $4n$ π electron counts on independent 10- and 20-cycles are compatible with an inner diatropic/outer paratropic pattern. The fact that the AWA picture predicts counter-rotating currents makes [10,5]-coronene a very peculiar molecule. Indeed, in coronene and corannulene, AWA is completely unable to account for the opposition of currents,[17]

[†] Dipartimento di Chimica, Università di Salerno.
[‡] Department of Chemistry, University of Sheffield.

10.1021/jp0600559 CCC: $33.50
Published on Web 05/23/2006

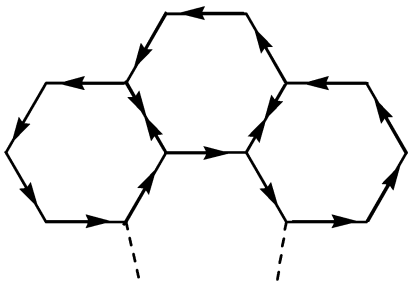

Figure 1. Scheme of ring currents in a circulene, showing the genesis of the central current from local ring currents in the external rings.

CHART 1. [10,5]-Coronene, 1

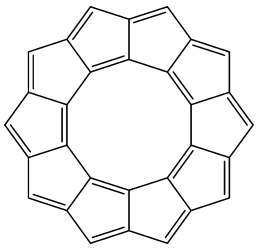

1

as it would predict concentric $(4n + 2)$ π cycles (if transfer of one electron to the central pentagon is invoked for corannulene) and hence conrotating diatropic currents in both molecules. In these systems, the radial bonds have Pauling bond order 8/20 and 5/11, respectively. Even a weak coupling between inner and outer cycles is known to be sufficient to upset the prediction of the AWA model,[17−19] so that this model is certainly not generally valid.

Another simple model, based on node counting, can be used to give an independent prediction of the sense and spatial distribution of the currents in **1**. The general ipsocentric orbital model[15,16] explains current in terms of characteristics of the frontier orbitals. In this formulation, induced current density of a planar π system subjected to a perpendicular external magnetic field can be partitioned into physically nonredundant contributions, expressed in terms of virtual transitions between occupied π and empty π^* orbitals, weighted by an energy denominator, and obeying selection rules which can be expressed in terms of symmetry and node counts. If the π/π^* orbital product spans the symmetry of an in-plane translation (if the transition adds one angular node), the contribution of the excitation to the induced current has the diatropic sense. If the symmetry product contains the representation of the in-plane rotation (the transition preserves the angular node count), the contribution has the paratropic sense.

A simple Hückel calculation suffices to obtain the nodal characteristics of the π frontier orbitals of **1** (Figure 2). The nondegenerate HOMO has five angular nodal planes. It arises as an in-phase combination between one of the two NBOs of the 20-cycle and the fully antibonding MO of the 10-cycle, and is concentrated on 10 alternate perimeter sites. The nondegenerate LUMO is the other NBO of the 20-cycle. It is localized entirely on perimeter sites, with nodes lying between those of the HOMO. The HOMO−LUMO excitation is thus of pure rotational character, leading to a paratropic current concentrated on the perimeter. Below the HOMO, but nearly degenerate with it, is a pair of orbitals with two angular nodes, arising from out-of-phase combination of two-node MOs of 10- and 20-cycles, with largest coefficients on the inner cycle. This HOMO-1 pair is linked by a node-increasing excitation to a LUMO+2 π^* pair that has three angular nodal lines on the inner cycle. The excitation between HOMO-1 and LUMO+2 pairs is therefore of pure translational character, leading to a diatropic current concentrated on the inner cycle. Thus, we have a definite prediction from node-counting, which in this particular case agrees with the AWA model, that the current-density map of [10,5]-coronene will be of the inverted paratropic-outside/diatropic-inside type, with the outer and inner currents arising respectively from two and four frontier π electrons.

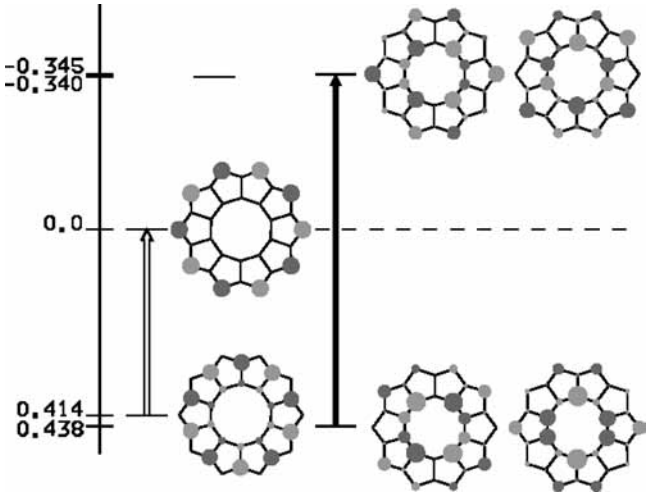

Figure 2. Hückel molecular orbital energy diagram for [10,5]-coronene, from HOMO-1 to LUMO+2. Orbital energies are displayed relative to α in units of β. Black and white arrows represent translational (diatropic) and rotational (paratropic) transitions respectively from occupied levels. The nodal characteristics of the orbitals corresponding to the Hückel π manifold are indicated schematically on the right of each level.

These clear semiempirical predictions are now confronted with the results of full ab initio calculations on [10,5]-coronene.

3. Ab Initio Calculations

The geometry of **1** was optimized using GAUSSIAN03[28] at the RHF/6-31G* and B3LYP/6-31G* levels. Initially the maximum possible D_{10h} symmetry was imposed, yielding structures with 4 (RHF) and 1 (DFT) imaginary frequencies; on relaxation along the imaginary-frequency mode of A_{2g} symmetry, the DFT calculations found a true local minimum of C_{10h} symmetry, but at the RHF level the symmetry fell further to C_{5h}. The descent from D_{10h} to C_{10h} predicted at the DFT level is consistent with a second-order Jahn−Teller interaction between HOMO and LUMO, B_{1g} and B_{2g} in D_{10h}, that become equisymmetric (B_g) in C_{10h}. The further symmetry breaking predicted at the RHF level may be unphysical, as in other macrocylic structures.[29] The B3LYP/6-31G* optimal structure, used in the further calculation of magnetic properties, has bond lengths 1.380 (inner CC), 1.486 (radial), 1.466 and 1.383 (perimeter), and 1.084 Å (CH), corresponding to partial double bonds on the 10π inner cycle, near-single bonds on the radial edges of the graph (as could be expected from their zero Pauling bond order) and a degree of bond fixation in the 20π outer cycle. The molecule is planar at equilibrium, but with low-frequency out-of-plane modes: in the B3LYP/6-31G* calculation, the (^{12}C,^{1}H) isotopomer has a nondegenerate mode at 34 cm^{-1} and doubly degenerate modes at 84, 191, and 192 cm^{-1}, all corresponding to out-of-plane distortions.

The 15 doubly occupied π orbitals of C_{10h} [10,5]-coronene span

$$B_g + 2E_{1g} + E_{3g} + 2A_u + 2E_{2u} + E_{4u},$$

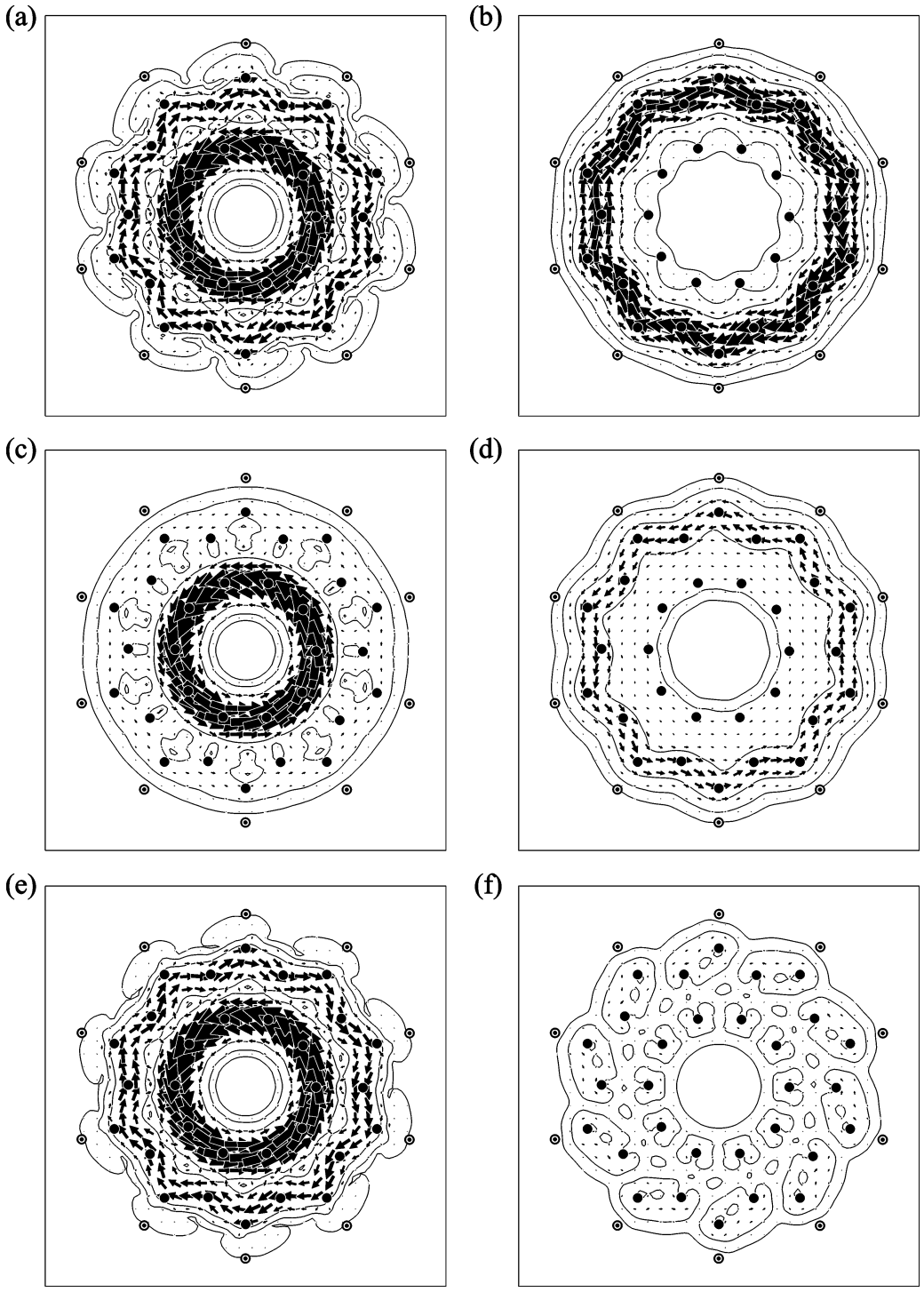

Figure 3. Maps of current density induced in the π system of the [10,5]-coronene molecule by a perpendicular external magnetic field. The current density is calculated at the ab initio CTOCD-DZ2/6-31G**//B3LYP/6-31G* level. Key: (a) total current density arising from the set of 15 π orbitals; contributions of (b) the B_g π HOMO, (c) the E_{2u} π HOMO-1 pair, and (d) the E_{4u} π HOMO-2 pair; sum of contributions from (e) the five highest-lying π orbitals (a + b + c) and (f) the 10 lowest-lying π orbitals (a−e). The plotting plane is $1a_0$ above that of the nuclei [(●) carbon; (○) hydrogen; positions projected into the plotting plane]. Contours indicate the magnitude of the total current density vector and arrows the direction and relative magnitude of its in-plane component. Diatropic/paratropic currents are represented by anticlockwise/clockwise sets of arrows.

with the 30 $1s^2$ cores and 50 CC- and CH-bonding σ orbitals spanning ν copies of

$$A_g + E_{2g} + E_{4g} + B_u + E_{1u} + E_{3u},$$

($\nu = 3$ for $1s^2$ cores and $\nu = 5$ for σ orbitals).

Current density maps were calculated in the ipsocentric approach at the CTOCD-DZ2/6-31G**//B3LYP/6-31G* level using the SYSMO program.[30] The maps show the calculated current density per unit field, induced by an external magnetic field oriented along the C_{10} axis, and plotted at a height of $1a_0$ from the molecular plane. Strengths of the different circulations can be judged by the value of j_{max}, the locally largest value of the current density per unit inducing magnetic field, quoted as a ratio to the corresponding quantity in the $1a_0$ plane for benzene, calculated using the same level of theory. (This "standard" benzene value is 0.08 au[21]). These strengths can also be judged by the value of the "current susceptibility" obtained

TABLE 1: HF and B3LYP Magnetic Properties Calculated Using 6-31G GIAO Basis Set at the B3LYP/6-31G* C_{10h} Geometry[a]**

	HF[b]			B3LYP[c]		
magnetic properties	⊥	∥	av	⊥	∥	av
σ ^{13}C inner ring	36	157	76	33	92	53
σ ^{13}C non-hydrogenated outer ring	−13	97	24	−14	52	8.3
σ ^{13}C hydrogenated outer ring	62	168	87	40	152	77
σ ^{1}H	25.0	29.0	26.3	26.8	38.7	30.8
magnetizability	−2425	−4234	−3028	−2175	10 013	1887

[a] Absolute shieldings in ppm, magnetizability in 10^{-30} J T^{-2}. [b] HF: LUMO−HOMO gap = 0.00245 − (−0.23535) = 0.2378 au. [c] B3LYP: LUMO−HOMO gap = −0.11587 − (−0.17813) = 0.06226 au.

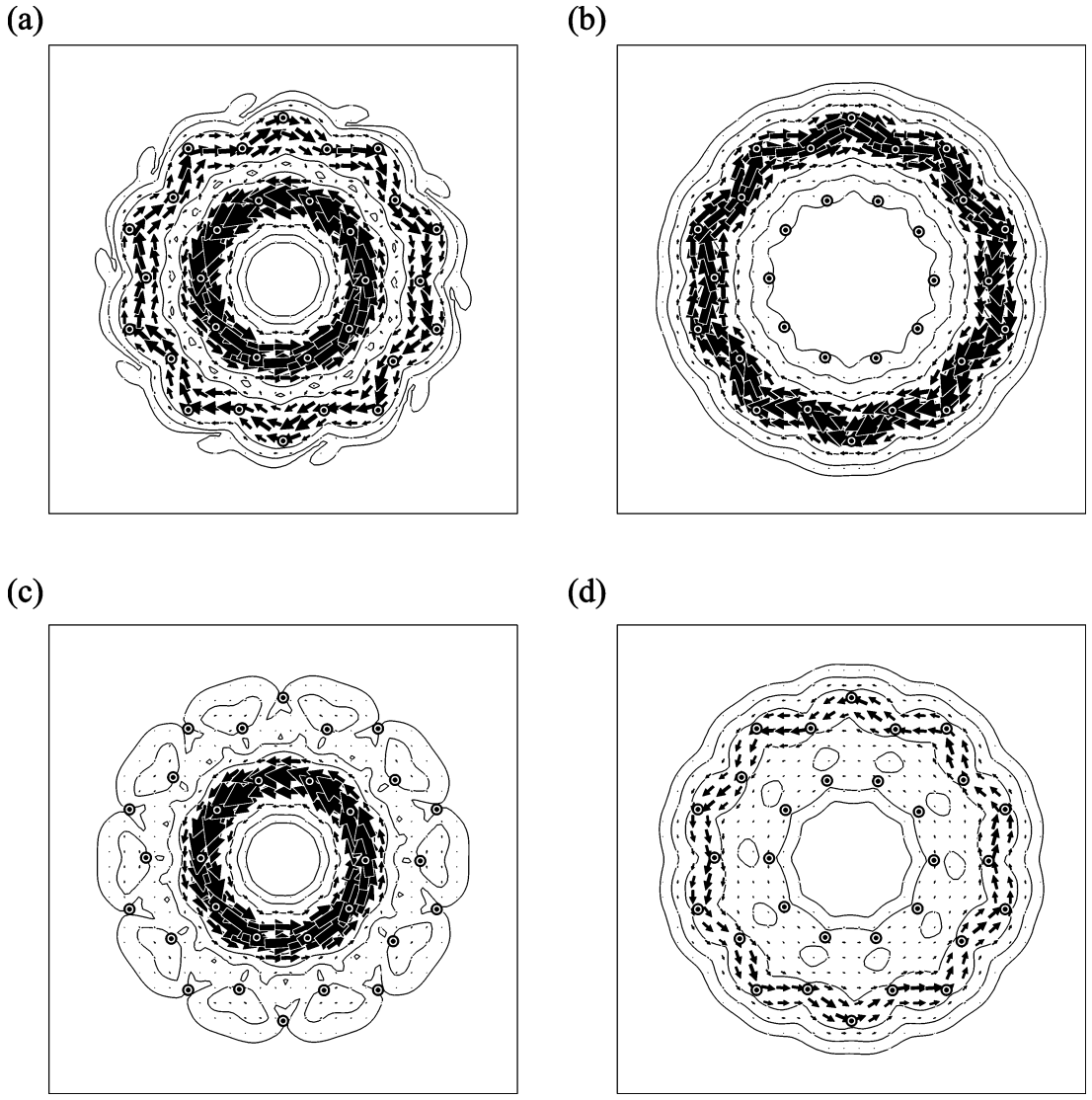

Figure 4. Maps of the current density induced in the π system of the [10,5]-coronene molecule by a perpendicular external magnetic field. The current density is calculated in the pseudo-π model at the B3LYP/6-31G* geometry. Key: (a) total current density arising from the set of 15 π orbitals; contribution of (b) the HOMO, (c) the HOMO-1 pair, and (d) the HOMO-2 pair. In the model, the plotting plane is that of the pseudo-hydrogen nuclei; other conventions are as in Figure 3.

integrating the current density per unit inducing magnetic field passing through a half-plane grid perpendicular to the molecular plane, working out from the central axis.[14] Conveniently, these current strengths can be quoted as a ratio to the corresponding quantity for benzene, calculated using the same level of theory. Averaging the current susceptibilities for the two grids corresponding to the Cartesian half planes, the CTOCD-DZ2/6-31G** benzene value is 11.24 nA T^{-1}, in good agreement with previous results.[14]

Figure 3 shows the total current arising from the set of 15 π orbitals, and the separate contributions to this total from the nondegenerate HOMO and the HOMO-1 and HOMO-2 pairs (the order of the near-degenerate B_g and E_{2u} levels is reversed at the RHF geometry). It is seen that the pattern of current is indeed inverted with respect to the normal circulenes, and that the two counter-rotating currents arise from the two different orbital-excitation mechanisms predicted on node-counting arguments.

The measures of current strength show that we are dealing with substantial ring currents. CTOCD-DZ2/6-31G** current susceptibility ratios are 1.19, 1.41, and 0.63 for the B_g π HOMO, E_{2u} π HOMO-1 pair, and E_{4u} π HOMO-2 pair, respectively.

The corresponding values of j_{max} are 1.12, 1.48, and 0.44. Thus, as shown in Figure 3, about half of the HOMO paratropic ring current is canceled by the diatropic current arising from the HOMO-2 pair. The resultant net paratropic circulation remains significant, amounting to more than half of the benzene ring current.

The maps are robust against geometric change and the ring currents that they predict have direct effects on out-of-plane tensor components of both magnetizability and proton shielding. Table 1 reports the full set of first-order magnetic properties of **1** calculated with the G03 package at both HF and B3LYP levels of approximation, using a 6-31G** GIAO basis set of and B3LYP/6-31G* C_{10h} geometry.

It can be seen that the B3LYP results give large enhancements of the paratropicity, dominated by the out-of-plane component and by the small (and probably badly underestimated[32]) DFT HOMO−LUMO gap. Other pure and hybrid density functionals give similar results. Thus, although we can be sure of the qualitative pattern in the maps, the exact balance of inner and outer currents is somewhat tricky to compute, and we therefore, do not see a way of making definitive predictions for the sign and size of the global magnetic properties of this molecule at these levels of theory.

4. Pseudo π Calculations

Pseudo-π modeling of a planar π system has two stages.[32] First, the conjugated carbon centers of the π system are replaced by a set of hydrogen atoms on the same positions, each consisting of a unit positive charge, bearing a single 1s (STO-3G) basis function and contributing a single electron. Then, the map of the current density induced in the H_N-system by a perpendicular magnetic field is calculated self-consistently and *ipsocentrically*, i.e., with the full coupled Hartree−Fock CTOCD-DZ (continuous transformation of origin of current density-diamagnetic zero) approach. The first stage rests on the one-to-one correspondence between the Hückel molecular orbitals of a π system and the σ orbitals of an array of hydrogen atoms with the same connectivity. Both are defined by eigenvectors of the same adjacency matrix, representing the same linear combinations of the respective basis functions, with the same energy eigenvalue expressions, adjusted appropriately for scale and origin. The symmetries of the orbitals are also related. In a planar system, each π molecular orbital of symmetry $\Gamma(\pi)$ is converted on switching p_π and s basis functions to a σ molecular orbital of symmetry $\Gamma(\sigma) = \Gamma(\pi) \times \Gamma_z$, where Γ_z is the symmetry of a translation perpendicular to the plane.

The correspondence of unperturbed π orbitals of C_N and σ orbitals of H_N implies that there should also be a one-to-one correspondence of orbital contributions to the total current density induced by a perturbing magnetic field. As the p_π to s switch corresponds in both planar and curved systems to multiplication of the orbital symmetry by a one-dimensional representation, the symmetries of $\pi \rightarrow \pi^*$ transitions are preserved, and the selection rules carry over unchanged. As a consequence, the pseudo-π model reproduces overall patterns and specific features of the current density maps for a wide range of planar systems; it also captures the breakdown of total π current into orbital contributions.[32] Qualitative questions about aromaticity of specific systems can therefore often be settled without recourse to expensive ab intio calculation

The model also benefits from an unexpectedly precise numerical coincidence. It turns out that when STO-3G hydrogen ls orbitals are used with typical carbon−carbon distances, there is a close *numerical* match between the σ currents calculated in the nuclear plane of H_N and the π currents calculated for C_N in the $1a_0$ plotting plane. The difference in pseudo-π and true π currents for benzene is less than 1%, for example.

Taking the calculated B3LYP/6-31G* geometry of the [10,5]-coronene, the pseudo-π model was applied directly: all carbon centers were replaced by hydrogen atoms bearing STO-3G 1s functions and current density was calculated in the ipsocentric approach. Figure 4 shows the maps of current density plotted in the molecular plane. As can be seen, the agreement with the ab initio current density maps is superb. In particular, each orbital contribution is very well reproduced, making it almost impossible to distinguish pseudo-π from ab initio plots.

5. Conclusions

Using recently introduced quantum mechanical methods for computing and visualizing current-density maps, the design of a new molecule supporting an inverted diatropic-hub/paratropic-rim pattern of induced currents has been successfully carried out. The proposed procedure can be easily generalized to other molecular systems. The study reveals that the combination of economical pseudo-π calculations, the ipsocentric model and simple chemical reasoning gives a powerful toolkit for the design of molecular ring-current patterns and ultimately of specific molecular properties.

References and Notes

(1) Keith, T. A.; Bader, R. F. W. *Chem. Phys. Lett.* **1993**, *210*, 223.
(2) Keith, T. A.; Bader, R. F. W. *J. Chem. Phys.* **1993**, *99*, 3669.
(3) Lazzeretti, P.; Malagoli, M.; Zanasi, R. *Chem. Phys. Lett.* **1994**, *220*, 299.
(4) Coriani, S.; Lazzeretti, P.; Malagoli, M.; Zanasi, R. *Theor. Chim. Acta* **1994**, *89*, 181.
(5) Zanasi, R.; Lazzeretti, P.; Malagoli, M.; Piccinini, F. *J. Chem. Phys.* **1995**, *102*, 7150.
(6) Zanasi, R. *J. Chem. Phys.* **1996**, *105*, 1460.
(7) Steiner, E.; Fowler, P. W. *Int. J. Quantum Chem.* **1996**, *60*, 609.
(8) Zanasi, R.; Lazzeretti, P.; Fowler, P. W. *Chem. Phys. Lett.* **1997**, *278*, 251.
(9) Fowler, P. W.; Steiner, E.; Zanasi, R.; Cadioli, B. *Mol. Phys.* **1999**, *96*, 1099.
(10) Ligabue, A.; Pincelli, U.; Lazzeretti, P.; Zanasi, R. *J. Am. Chem. Soc.* **1999**, *121*, 5513.
(11) Steiner, E.; Fowler, P. W.; Viglione, R. G.; Zanasi, R. *Chem. Phys. Lett.* **2002**, *355*, 471.
(12) Viglione, R. G.;, Zanasi, R. *Phys. Chem. Chem. Phys.* **2004**, *6*, 295.
(13) Soncini, A.; Fowler, P. W.; Lazzeretti, P.; Zanasi, R. *Chem. Phys. Lett.* **2005**, *401*, 164.
(14) Jusélius, J.; Sundholm, D.; Gauss, J. *J. Chem. Phys.* **2004**, *121*, 3952.
(15) Steiner, E.; Fowler, P. W. *J. Phys. Chem. A* **2001**, *105*, 9553.
(16) Steiner, E.; Fowler, P. W. *Chem. Commun.* **2001,** 2220.
(17) Steiner, E.; Fowler, P. W.; Jenneskens, L. W. *Angew. Chem., Int. Ed.* **2001**, *40*, 362.
(18) Steiner, E.; Fowler, P. W.; Jenneskens, L. W.; Acocella, A. *Chem. Commun.* **2001**, 659.
(19) Acocella, A.; Havenith, R. W. A.; Steiner, E.; Fowler, P. W.; Jenneskens, L. W. *Chem. Phys. Lett.* **2002**, *363*, 64.
(20) Johansson, M. P.; Jusélius, J.; Sundholm, D. *Angew. Chem., Int. Ed.* **2005**, *44*, 1843.
(21) Fowler, P. W.; Havenith, R. W. A.; Jenneskens, L. W.; Soncini, A.; Steiner, E. *Angew. Chem., Int. Ed.* **2002**, *41*, 1558.
(22) Fowler, P. W.; Zanasi, R.; Cadioli, B.; Steiner, E. *Chem. Phys. Lett.* **1996**, *251*, 132.
(23) Fowler, P. W.; Steiner, E.; Cadioli, B.; Zanasi, R. *J. Phys. Chem. A* **1998**, *102*, 7297.
(24) Zanasi, R.; Fowler, P. W. *Chem. Phys. Lett.* **1995**, *238*, 270.
(25) Pasquarello, A.; Schlüter, M.; Haddon, R. C. *Science* **1992**, *257*, 1660.
(26) Bochvar, D. A.; Gal'pern, E. G.; Gambaryan, N. P. *Izv. Akad. Nauk SSSR, Ser. Khim.* **1970**, *2*, 435.
(27) Aihara, J. *J. Am. Chem. Soc.* **1992**, *114*, 865.
(28) Gaussian 03, Revision B.05, Frisch, M. J.; Trucks, G. W.; Schlegel, H. B.; Scuseria, G. E.; Robb, M. A.; Cheeseman, J. R.; Montgomery, J. A., Jr.; Vreven, T.; Kudin, K. N.; Burant, J. C.; Millam, J. M.; Iyengar, S. S.;

Tomasi, J.; Barone, V.; Mennucci, B.; Cossi, M.; Scalmani, G.; Rega, N.; Petersson, G. A.; Nakatsuji, H.; Hada, M.; Ehara, M.; Toyota, K.; Fukuda, R.; Hasegawa, J.; Ishida, M.; Nakajima, T.; Honda, Y.; Kitao, O.; Nakai, H.; Klene, M.; Li, X.; Knox, J. E.; Hratchian, H. P.; Cross, J. B.; Bakken, V.; Adamo, C.; Jaramillo, J.; Gomperts, R.; Stratmann, R. E.; Yazyev, O.; Austin, A. J.; Cammi, R.; Pomelli, C.; Ochterski, J. W.; Ayala, P. Y.; Morokuma, K.; Voth, G. A.; Salvador, P.; Dannenberg, J. J.; Zakrzewski, V. G.; Dapprich, S.; Daniels, A. D.; Strain, M. C.; Farkas, O.; Malick, D. K.; Rabuck, A. D.; Raghavachari, K.; Foresman, J. B.; Ortiz, J. V.; Cui, Q.; Baboul, A. G.; Clifford, S.; Cioslowski, J.; Stefanov, B. B.; Liu, G.; Liashenko, A.; Piskorz, P.; Komaromi, I.; Martin, R. L.; Fox, D. J.; Keith, T.; Al-Laham, M. A.; Peng, C. Y.; Nanayakkara, A.; Challacombe, M.; Gill, P. M. W.; Johnson, B.; Chen, W.; Wong, M. W.; Gonzalez, C.; Pople, J. A. Gaussian, Inc.: Wallingford CT, 2004.

(29) Baker, J.; Kozlowski, P. M.; Jarzecki, A. A.; Pulay, P. *Theor. Chem. Acc.* **1997**, *97*, 59.

(30) Lazzeretti, P.; Malagoli, M.; Zanasi, R. SYSMO Package, University of Modena. Steiner, E.; Fowler, P. W.; Havenith, R. W. A.; Soncini, A. additional routines for the evaluation and plotting of current density, University of Exeter.

(31) Allen, M. J.; Keal, T. W.; Tozer, D. J. *Chem. Phys. Lett.* **2003**, *380*, 70 and references therein.

(32) Fowler, P. W.; Steiner, E. *Chem. Phys. Lett.* **2002**, *364*, 259.